THE PEOPLE'S DEMOCRATIC REPUBLIC OF ALGERIA
THE MINISTRY OF HIGHER EDUCATION AND SCIENTIFIC RESEARCH

AMAR TELIDJI UNIVERSITY OF LAGHOUAT
FACULTY OF TECHNOLOGY
DEPARTMENT OF ELECTROTECHNIC

Master's dessertation

Domain :Science And Technology
Field : Electrotechnic
Option :Electric Control

Theme

Improved Sensorless Speed Vector Control Of Induction Motor Drive Based On Synergetic Theory

---

Presented by :
REZGALLAH CHAIMA

chairman:	*BIRANE Mouhoub*	M .C. A
Examiner:	*BESSEDIK Sid Ahmed*	Professor
Supervisor:	*KOUZI Kattia*	Professor

Academic year 2023/2024

Acknowledgements

Praise be to the Almighty God who has granted me faith, courage, and patience to complete this work.

Secondly, I would like to express my deep gratitude to my dear supervisor, Mrs. Katia KOUZI from Laghouat University, who has been like a second mother to me, for her patience, guidance, and encouragement. She truly provided me with the support I needed, and I pray that Allah blesses her.

A special mention must also go to the members of the jury. I would like to thank everyone who assisted me in improving my work and provided feedback that helped refine this manuscript.

Lastly, but not least, I would like to thank all the teachers and administrative staff in our department and all my friends from the class of 2019 to 2024.

Finally, I express my gratitude to all those who have contributed in one way or another to the development of this work.

Rezgallah Chaima

Dedication

I dedicate my humble effort to my beloved father Ahmed and mother Fatima, and to my teacher Katia, whose love and prayers enabled me to achieve this success.

To my dear sister Fatima Zahra, who has been a support throughout my academic journey until this moment.

To my brother's dear wife Aisha.

to all my brothers and sisters without exception.

Rezgallah Chaima

الملخص:

الهدف الرئيسي من هذه الدراسة هو تعزيز أداء التحكم في السرعة بدون حساس المتكامل لمحرك الحث(IM)في الجزء الأول من هذا العمل، قمنا بنمذجة محرك الحث ومصدر الطاقةالخاص به الذي يتكون أساسًا من محول جهد يتم التحكم فيه بواسطة تيار مع تقنية(PWM) الهستيرية، ثم قدمنا جانب التحكم الاتجاهي المطبق على محرك الحث. في المرحلة الثانية، تم اقتراح استراتيجيتين للتحكم، وهما التحكم الاتجاهي الضبابي والتحكم الاتجاهي المتكامل المطبق على محرك الحث. تم توضيح والتعليق على العديد من نتائج المحاكاة العددية للأوامر المقدمة. في المرحلة الأخيرة، ولتقليل ظاهرة التقطيع، تم تطوير التحكم في السرعة بدون حساس لمحرك الحث المزود بمراقب انزلاقي تكيفي محسّن. فكرة المراقب المقترح هي استبدال مصطلح المراقب التبديل للمراقب الانزلاقي التكيفي التقليدي بوظائف ناعمة والاحتفاظ بالمزايا التي تحققت من هذا الأخير. يقدر المراقب مكونات التدفق الدوار في إطار الإشارة الثابتة بواسطة قياس محرك الحث. يتم تقدير السرعة الميكانيكية بإضافة دالة ليابونوف. تم توضيح كفاءة وأداء خوارزمية التقدير المقدمة من خلال نتائج المحاكاة.

الكلمات المفتاحية : محرك الحث(IM) ؛ التحكم الاتجاهي؛ منظمPI ؛ التحكم التآزري، المراقب الانزلاقي التكيفي المحسن، دالة ليابونوف، دالة ناعمة، المتانة

Abstract :

The main objective of this memory is to enhance the performance of synergetic sensorless speed vector control of Induction Motor (IM). In the first part of this work, we have modeled the induction motor and its power supply consists mainly of voltage inverter controlled by current with hysteresis PWM, then we have presented the aspect of vector control applied to IM. In the second phase, two control strategies were proposed, namely fuzzy and synergetic vector control applied to the IM. Several numerical simulation results ofthe presented command were illustrated and commented on. In the last phase, in order to minimize the chattering phenomena, it was developedsensorless speed vector control of IM equipped with an improved adaptive sliding mode observer. The idea of proposed observer is replace the switching observer term of conventional adaptive sliding mode observer by smooth functionsand retain the benefits achieved by this later. The observer estimates the rotor flux components in the stationary reference frame by the IM measurement. The mechanical speed is estimated by adding a Lyapunov function. The performance and efficiency of the presented estimation algorithm were illustrated by simulation results.

Keywords- Induction Motor (IM); Vector Control; PI regulator; Synergetic Control, Improved Adaptive Sliding Mode Observer, Lyapunov function, Smooth Function, Robustness.

Résumé :

L'objectif principal de ce mémoire est d'améliorer les performances d'un contrôle vectorielsynergétique sans capteur de vitesse d'un moteur à induction triphasé (MI). La première partie de ce travail, on a modélisé le moteur à induction et son alimentation constituée principalement par un onduleur de tension commandé en courant par MLI à hystérésis, puis on a présenté la technique de la commande à flux orienté et son application au MI. Dans une deuxième phase, on a exposé deux stratégies de commande à savoir lacommande découplée floue et synergétique appliquées au MI. Plusieurs résultats de simulation numérique de deux contrôles présentés ont été illustrés et commentés. Dans la dernière phase, afin de minimiser le phénomène de broutement 'chattering' on a développé un contrôle vectoriel sans capteur de vitesse du MI associé d'un observateur adaptatif à mode glissement amélioré. L'idée de l'observateur proposé est de remplacer le terme discontinu de l'observateur adaptatif à mode glissement conventionnel par des fonctions adoucies tout enretient les avantages de ce dernier.

L'observateur estime les flux rotoriques dans le référentiel lié au stator à partir les mesures du moteur. La vitesse de rotation mécanique est estimée par l'ajout d'une fonction de Lyapunov. Les performances et l'efficacité de l'algorithme de commande proposée ont été illustrées par des résultats de simulation.

Mots clés : Moteur à Induction triphasé, Commande vectorielle, Régulateur PI classique, Contrôle synergétique, Observateur à Modes glissants Adaptatif Amélioré,Fonction de Lypunov, Fonction adoucie, Robustesse.

Contents

List of Figures

List of Symbols

- C_e: Electromagnetic torque (N.m)
- C_r: Resistance torque (N.m)
- f: Network frequency (Hz)
- i_{dqs}: Components of stator, direct and quadrature current (A)
- i_{dqr}: Components of rotor, direct and quadrature (A)
- $i_{\alpha\beta s}$: Composantes du courant statorique dans le référentiel du stator (A)
- J: Moment of inertia (Kgm^2)
- k: Discrete moment (t)
- k_1, k_2: Observer gains by sliding modes (without unity)
- K_p, K_i: Classical PI regulator coefficients (without unity)
- $k_e, k\Delta e, k\Delta cem$: Fuzzy PI regulator coefficients (without unity)
- $k_e1, k\Delta e1, kCem1$: Fixed adaptation gains of the blurred gains regulator adapted fuzzy (without unity)
- L_r: Circular cyclic inductance (H)
- L_s: Statoric cyclic inductance (H)
- f_r: Coefficient of friction (N.s)
- C: Filter capacity (F)
- L: Filter inductance (H)
- L_r: Circular cyclic inductance (H)

- M: Mutual cyclic inductance (H)
- Ω: Rotor mechanical rotation speed (tr/mn)
- ω_g: Sliding pulse (rad/s, tr/mn)
- ω_s: Stator pulsation (rad/s, tr/mn)
- ω_r: Rotor angular speed of rotation (rad/s, tr/mn)
- p: Number of pole pairs (without unity)
- Ψ_{dqs}: Components of stator, direct and quadrature flux (Wb)
- $\Psi_{\alpha\beta s}$: Components of the rotor flux in the stator (Wb)
- R_r: Resistance of a rotor phase (Ω)
- R_s: Resistance of a stator phase (Ω)
- σ: Coefficient of dispersion of Blondel (without unity)
- σ_r: Rotor time inverse constant (s^{-1})
- Tech: Sampling period (s)
- T_r: Rotor time constant (s)
- θ: Rotor mechanical rotation angle (rad)
- θ_s: Electrical position of the referential rotating in relation to the stator (rad)
- $\hat{}$: Sign of an estimated size (without unity)
- ref: Sign of a reference quantity (without unity)
- $\hat{x}$: Estimated state
- v_{dqs}: Components of Stator, Direct and Quadrature Voltage (V)
- v_{dqr}: Components of rotoral, direct and quadrature voltage (V)
- $v_{\alpha\beta s}$: Stator voltage components in the stator reference (V)

GENERAL INTRODUCTION

PROBLEM FORMULATION

machines are widely used in industrial applications involving electromechanical energy conversion due to their favorable attributes such as low cost, reasonable size, robustness, and low maintenance. Many of these applications require the use of adjustable speed drives and a suitable control system that provides a large operating range and high dynamic and static performance [25].

The most popular used techniques are vector and direct torque controls. Decoupled control provides good performance during transient and permanent phases. IM operate primarily through vector control using classical regulators like PI, PD, and PID, which enables easy implementation and simple synthesis. However, these regulators have limitations when applied to IM due to their sensitivity to parameter variations, leading to reduced robustness.

The nonlinear controllers are introduced as solutions for the inconvenience of the linear regulators to improve the performance, robustness, and insensitivity to parameter variations. Recently the synergetic control earns its place in the robust control community as well the industrial partners and that after the successful implementation in power electronics [10].

The main features of synergetic control theory (SCT) are that it supports all parametric and nonparametric uncertainties, which is not possible in several control techniques. Also, synergetic control yields fast response, asymptotic stability of the closed-loop system in the all range operating condition, and system robustness in presence of parameter variation [8]. Moreover, the implementation of vector control algorithm requires the knowledge of rotor position and flux angle, which are generally obtained by a mechanical shaft sensor. The cost and reliability advantages of eliminating mechanical sensors and cabling for the measurement of position velocity and flux has led to active research into what is commonly termed “sensorless” or “self-sensing” control of induction machine[20].

Sensorless control must be used to lower the cost and volume of the drive system while increasing its reliability. In the literature, various types of research have been presented on the speed sensorless IM drive[19].

Sliding mode observers seems an attractive choice, in terms of robustness against parameter variations, external disturbance, and fast convergence[21].

However, the conventional sliding observer based on the variable structure control theory has some drawback such that the estimated values include high frequency chattering. This latter is due to the finite feedback gain and the discontinuous control input results in torque chattering which excites the high unmodeled dynamics or mechanical resonances. To overcome this problem, various solutions have been proposed in order to make a compromise between the chattering phenomenon minimization and observer robustness.Regarding of above point, we propose in this work simple but powerful improved sliding

Based on above point, in this work we present an improved sensorless synergetic decoupled control of induction motor based on an adaptive sliding-mode observer.

OUTLINE OF THE THESIS

The thesis is constructed by three chapters given as follows:

The first chapter of thesis is dedicated to modeling of IM in d.q reference frame, and its power supply composed by voltage inverter with PWM control. Besides, the application of indirect of vector control to IM will well explained. At the end of chapter, the performances of vector control will be given by simulation results.

The second chapter is dedicated to design of different robust controllers of IM speed regulation .We will use two kind of regulators such as:PI, synergetic controller (SC). Different digital simulation will be given to confirm this assertion.

The last chapter deal with the conception of an improved adaptive sliding-mode observer for speed-sensorless control of IM. The suggested observer estimate the rotor flux components in the stationary reference frame from IM. The speed is estimated by adding a Lyapunov function.

The effectiveness of the proposed estimation algorithm was evaluated under various operating conditions using a specific sensorless IM benchmark and the MATLAB/Simulink software environment.

To close this work, a general conclusion will be given, in regard to the continuation of this work, different perspectives will be suggested.

Chapter 1

Modeling and Vector Control of Induction Motor

1.1 Introduction

The asynchronous motor (MAS) or induction motor is currently the most widely used electric-motor in industry. Its main advantage lies in the absence of sliding electrical contacts, which leads to a simple and robust structure that is easy to build[12] . Its use in the field of variable speed drive calls upon the control, and to do this, one needs the mathematical model of the process. Thusthe modeling of the three-phase induction machine, an essential element in the drive, becomes an essential step for the realization of a variable speed control.

1.2 induction motor model

The mathematical model of an electric machine serves as a representation of the actual machine, enabling the simulation of experimentally observable behaviors. This model is instrumental in addressing technical challenges related to induction motors and significantly aids in their analysis and design.

1.2.1 IM modelling in the three-phase plan abc

Let a three-phase induction machine with stator and rotor represented schematically by the following figure:

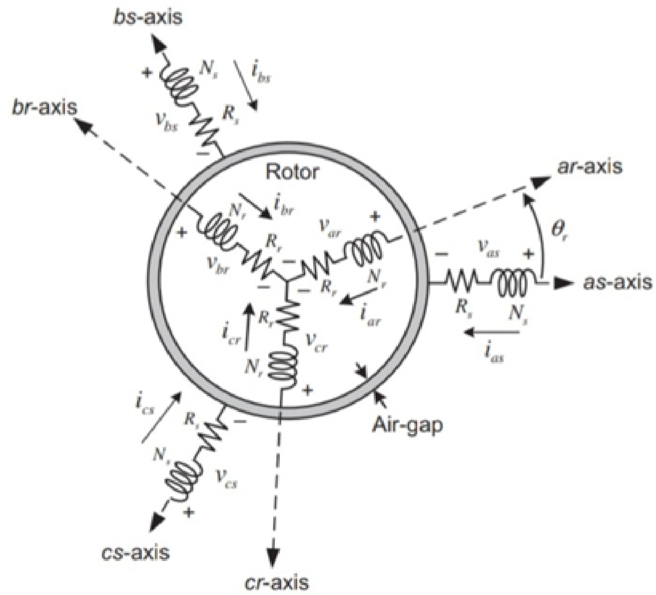

Figure 1.1: Schematic representation of a three-phase induction motor

The voltage equations

For the stator

$$[U_{sabc}] = R_s[i_{sabc}] + [L_s]\frac{d}{dt}[i_{sabc}] + \frac{d}{dt}\{[L_s][i_{rABC}]\} \tag{1.1}$$

For the rotor

$$[U_{rABC}] = R_r[i_{rABC}] + [L_r]\frac{d}{dt}[i_{rABC}] + \frac{d}{dt}\{[L_{sr}][i_{sabc}]\} \tag{1.2}$$

These equations reveal the relationship between variables, highlighting the inherent non-linearity that makes controlling the induction motor (IM) challenging. To address this issue, we employ the Park transformation.

1.3 Application of the park transformation on three-phase induction motor

Park's transformation aims to treat a wide range of machines in a unified way into a unique model. This conversion is often called axis transformation, corresponding fact at the two windings of the original machine followed by a rotation, the equivalent windings from an electrical and magnetic point of view. This transformation thus, for the purpose of making mutual inductances of the model independent of the angle of rotation[3].. The transformation that reflects this transition from the three-phase system to the two-phase system (d, q) is called Park, and given by:

$$[U_{dqo}] = [A][U_{abs}] \tag{1.3}$$

$$[i_{dqo}] = [A][i_{abs}] \tag{1.4}$$

$$[\psi_{dqo}] = [A][\psi_{abs}] \tag{1.5}$$

With [A]:is the park matrix

$$[A] = \begin{bmatrix} \cos\theta & \cos(\theta - 2\frac{\pi}{3}) & \cos(\theta + 2\frac{\pi}{3}) \\ -\sin\theta & -\sin(\theta - 2\frac{\pi}{3}) & -\sin(\theta + 2\frac{\pi}{3}) \\ \frac{1}{2} & \frac{1}{2} & \frac{1}{2} \end{bmatrix}$$

1.3.1 State form of the induction motor model in the mark (d, q) Linked to the rotating field

Under the assumptions of magnetic circuits linearity, and assuming sinusoidal distributed air-gap flux density, the equivalent two-phase model of induction motor, represented in a synchronous frame (d,q) and expressed in state-space form, is a fourth-order model [16]:

$$\dot{x} = Ax + Bv_s \tag{1.6}$$

where

$$x = [i_s^T \psi_r^T]^T, i_s = [i_{ds} i_{qs}]^T, \psi_r = [\psi_{dr} \psi_{qr}]^T, V_s = [V_{ds} V_{qs}]^T$$

The system matrices are given by:

$$A = \begin{bmatrix} -\frac{1}{\sigma L_s}(R_s + \frac{M^2}{L_r}\sigma_r) & \omega_s & \frac{M}{\sigma L_s L_r}\sigma_r & \frac{PM\Omega_r}{\sigma L_s L_r} \\ -\omega_s & -\frac{1}{\sigma L_s}(R_s + \frac{M^2}{L_r}\sigma_r) & -\frac{PM\Omega_r}{\sigma L_s L_r} & \frac{M}{\sigma L_s L_r}\sigma_r \\ M\sigma_r & 0 & -\sigma_r & (\omega_s - P\Omega_r) \\ 0 & M\sigma_r & -(\omega_s - P\Omega_r) & -\sigma_r \end{bmatrix}$$

$$B = \begin{bmatrix} \frac{1}{\sigma L_s} & 0 \\ 0 & \frac{1}{\sigma L_s} \\ 0 & 0 \\ 0 & 0 \end{bmatrix}$$

where
$\sigma = 1 - \frac{M^2}{L_s L_r}$ *and* $\sigma_r = \frac{R_r}{L_r}$.
The mechanical modeling part of the system is given by:

$$J\frac{d\Omega_r}{dt} = C_{em} - T_l - K_f\Omega_r \tag{1.7}$$

$$C_{em} = \frac{3}{2}P\frac{M}{Lr}(\psi_{dr}i_{qs} - \psi_{qr}i_{ds}) \tag{1.8}$$

1.3.2 Model of induction motor in mark linked to the stator

$$\frac{d}{dt}\begin{bmatrix}\hat{i_s} \\ \bar{\psi}\end{bmatrix} = \begin{bmatrix}A_{11} & A_{12} \\ A_{21} & A_{22}\end{bmatrix}\begin{bmatrix}\hat{i_s} \\ \bar{\psi}\end{bmatrix} + \begin{bmatrix}b \\ 0\end{bmatrix}\bar{V_s}$$

Or in vector

$$\frac{dx}{dt} = Ax + Bv_s \qquad \textit{State} \quad \textit{equation.} \tag{1.9}$$

$$y = \bar{i_s} = Cx \qquad \textit{Output} \quad \textit{equation.} \tag{1.10}$$

$$\bar{x} = \begin{bmatrix}\bar{i_s} \\ \bar{\psi}\end{bmatrix} \qquad \textit{State} \quad \textit{vector.}$$

with

$\bar{i_s} = \begin{bmatrix}i_{s\alpha} \\ i_{s\beta}\end{bmatrix}$ Stator current vector.

$\bar{\psi}r = \begin{bmatrix}\psi_{r\alpha} \\ \psi_{r\beta}\end{bmatrix}$ Rotor current vector.

$\bar{v_s} = v_s = \begin{bmatrix}v_{s\alpha} \\ v_{s\beta}\end{bmatrix}$ State voltage vector.

$a_{r11} = -(\frac{R_s}{\sigma L_s} + \frac{M^2\sigma_r}{\sigma L_s L_r})$
$A_{11} = a_{11}I$

$A_{12} = \frac{M}{\sigma L_s L_r}(\sigma_r I - \omega_r J) = a_{r12}I - a_{i12}J$

$A_{21} = a_{r21}I, a_{r21} = \sigma_r M,$

$A_{22} - \sigma I + \omega_r J = a_{r22}I + a_{i22}J, I = \begin{bmatrix}1 & 0 \\ 0 & 1\end{bmatrix}, J = \begin{bmatrix}0 & -1 \\ 1 & 0\end{bmatrix}$

$$b = b1I, \begin{bmatrix} b_1 \\ 0 \end{bmatrix}, b_1 = \frac{1}{\sigma L_s}$$

$\begin{bmatrix} I & 0 \end{bmatrix}$ Output Matrix; I and 0: Identity and dim zero matrices 2*2.

1.3.3 Modeling of the induction motor -voltage inverter association

The inverter is a static converter capable of transforming the electrical energy of a source ofdirect voltage in an alternating type electrical energy, the use of inverters is very extensive in the industry, such as variable speed drives for three-phase motor, induction motor...etc. see Figure:

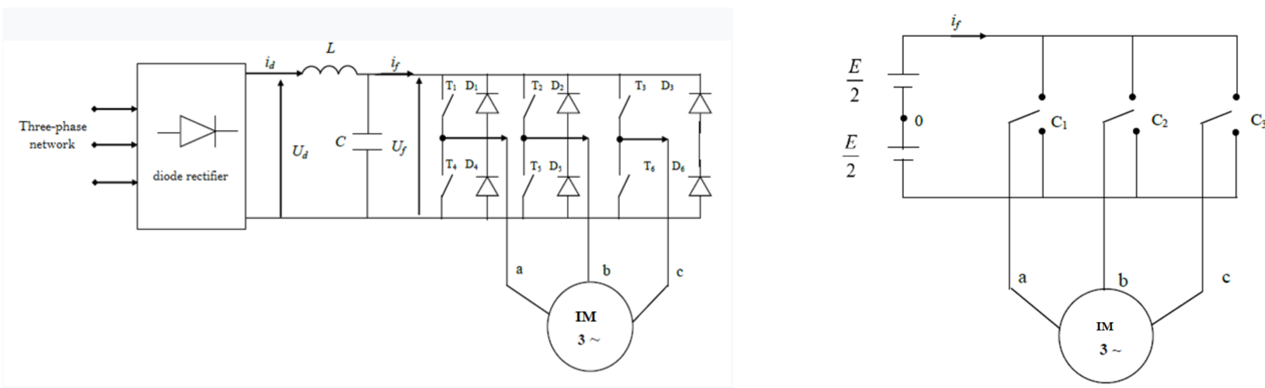

Figure 1.2: Diagram of the induction motor- voltage inverter by switches association

Each switch C is associated with a logic function F_i with (i=1.3), such as: If F_1 = 1 then phase a is connected to the positive terminal of the DC source E. And F_1 = -1 then phase a is connected to negative terminal of DC source E.
Then

$$U_{ab} = \frac{1}{2}(F_1 - F_2)E$$
$$U_{bc} = \frac{1}{2}(F_2 - F_3)E$$
$$U_{ca} = \frac{1}{2}(F_3 - F_1)E$$

The current at the input of the inverter has the expression:

$$i_f = F_1 i_a + F_2 i_b + F_3 i_c \tag{1.11}$$

1.3.4 Hysteresis MLI control

The hysteresis control method in multilevel inverters (MLIs) ensures that the phase current closely tracks the reference current, thereby guaranteeing a constant electromagnetic torque on the asynchronous machine. This control approach involves comparing the measured phase current with the reference current using a hysteresis comparator. The comparator generates pulses to trigger and block the inverter switches, effectively limiting the phase current within a hysteresis band of $2\Delta i$ around the reference current [20].. The switching conditions of the three static switches Fi (i=1,3) of the inverter are determined based on their corresponding logical states. This strategy simplifies the control process and maintains stable operation of the system as follows:

$$Fi = -1 \;\; if \;\; i_i \geq i_{ref} + \Delta i \tag{1.12}$$

$$Fi = 1 \;\; if \;\; i_i \leq i_{ref} - \Delta i \tag{1.13}$$

$$Fi = F_{(i-1)} \;\; i_i = i_{ref} \tag{1.14}$$

With i (i=1, 3): are the currents of the stator phases (ia,ib,ic).
i_{ref} (i=1, 3): are the reference currents from the three inverter arms.
Δi: The hysteresis band is selected to ensure the switching frequency of the controlled semiconductor remains within permissible limits while also minimizing current harmonics effectively..

1.3.5 Simulation results and discussion

The differential equations in state space and the dynamic equation were numerically solved using MATLAB software. The simulation utilized the parameters of the induction motor (IM) as provided in the appendix (A). Two tests were conducted and are presented below:

1.3.6 Operating without load

Figure (1.3) shows the evolution of the characteristics of the IM without load operation (Tr=0) :

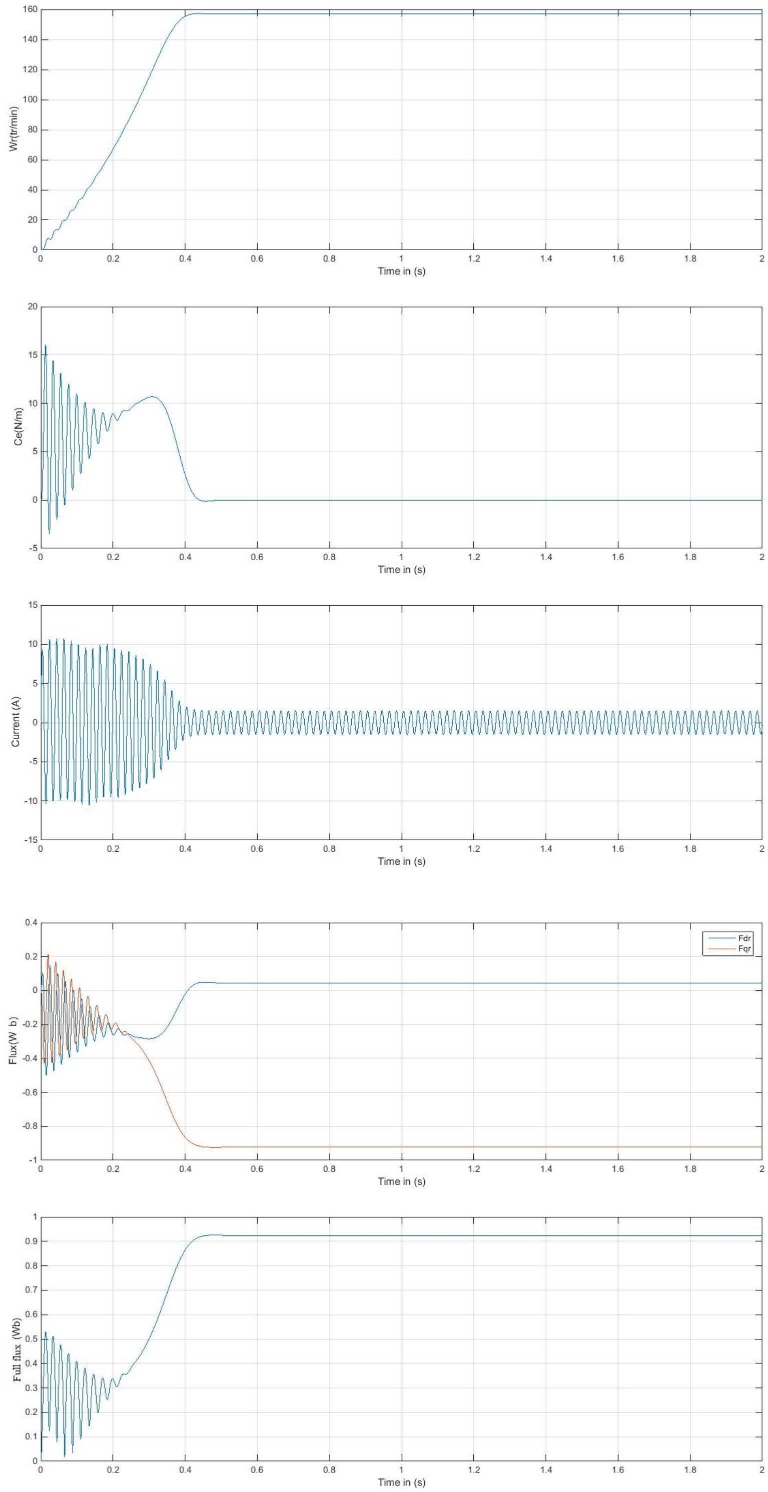

Figure 1.3: Dynamic and static Characteristic of IM without load torque

1.3.7 Operating with load Tr=5 N.m

In this test, we introduce load torque $T_r = 5$ N.m at t = [0.8,1.2]s

Simulation results and discussion of induction motor modelling with load

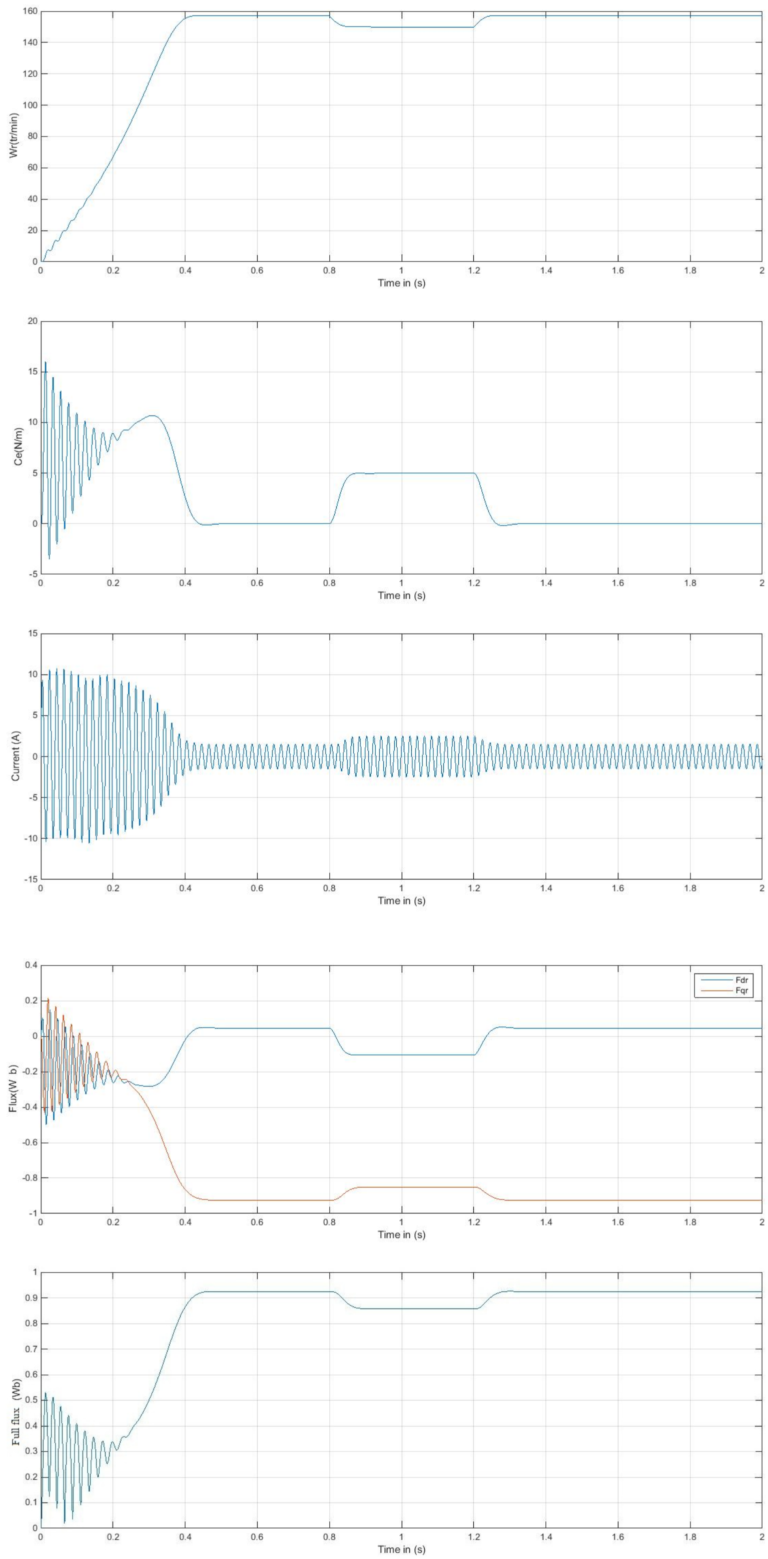

Figure 1.4: IM characteristic during load application Tr= 5N.m at t = [0.8-1. 2]s

Discussion

These figures demonstrate a relationship between torque and flux, which is the cause of the motor's non-linearity. To address this, we use vector control to decouple torque and flux, thereby mitigating the non-linearity issue.

1.4 IM Control technique

1.4.1 Introduction

Induction motor control has been a focal point of research and development over the past few decades. Among the notable advancements in this field is Vector Control (VC), which employs partial feedback linearization in conjunction with a proportional integral (PI) controller to manage the motor's state. The upcoming section will delve into the fundamental aspects of vector control and its implementation in induction motors..

1.4.2 Principle of flux orientation control (F.O.C)

The examination of asynchronous machine torque expression reveals that it arises from the product difference of two orthogonal components: the rotor flux and stator currents, which exhibit complex interdependencies between machine variables. The goal of flux-oriented control is to decouple these quantities responsible for magnetizing the machine and producing torque.

Mathematically, the control law aims to transform the system from one with inherent dual nonlinearity into a linear system that ensures independence between flux creation and torque production, similar to a separately excited DC machine. Flux-oriented control involves adjusting flux using one current component and torque using another. This necessitates choosing a "d, q" axis system.

A strategic selection of the "d, q" axis orientation angle aligns the "d" axis with the resultant flux, thereby eliminating the transverse flux component. The reference axes can be chosen based on one of the machine fluxes, such as the stator flux, rotor flux, or air-gap flux. This choice dictates the conditions for orienting the machine axes to achieve optimal control

Stator flux

$$\phi_{ds} = \phi_s \qquad and \qquad \phi_{qs} = 0 \tag{1.15}$$

Air gap flux

$$\phi_{dr} = \phi_r \qquad and \qquad \phi_{qm} = 0 \tag{1.16}$$

Rotor flux

$$\phi_{dr} = \phi_r \qquad and \qquad \phi_{qr} = 0 \tag{1.17}$$

In the three reference systems, the torque is proportional to the flux product by the current component iqs but only the choice of rotoric flux allows a decoupling characterized by an independence of flux and current component in quadrature with flux, Moreover, this choice makes it possible to have a high starting torque which justifies the use of this type of flux orientation[17].

1.4.3 Vector control types

There are two main types of vector control -The direct vector control. - The indirect vector control.

The direct vector control

This control method was proposed by Blaschke. In this case, the knowledge of the flux module and its phase is required to ensure decoupling between torque and flux regardless of the point of operation in order to access information concerning the amplitude and phase of the flux, it is possible to use sensors. The disadvantage of this method is that the sensors are mechanically fragile and cannot work under severe conditions such as vibration and excessive heating.

The indirect vector control

The principle of this method consists in not measuring (or estimating) the amplitude of flux but only its position, the idea is proposed by Hasse. It consists in estimating the position of the flux vector. This method has been favoured by the development of microprocessors, it is very sensitive to the parametric variations of the machine. It is important to note that the indirect method is the simplest and most used than the direct method, but the choice between the two methods varies from application to application[14].

1.4.4 Induction Motor Current Model

When the presence of the frequency converter is unknown, assuming it is ideal, and the effect of the stator dynamic, we obtain the model of the induction motor current: This phenomenon put the AC machine as the perfectly compounded separate excitation content current machine or there is a natural decoupling between torque and flux.

1.4.5 Speed regulation of the IM controlled vector by a conventional PI

The block diagram of the speed control of a drive based on the asynchronous flUX machine oriented by a conventional PI controller is represented by the following figure:

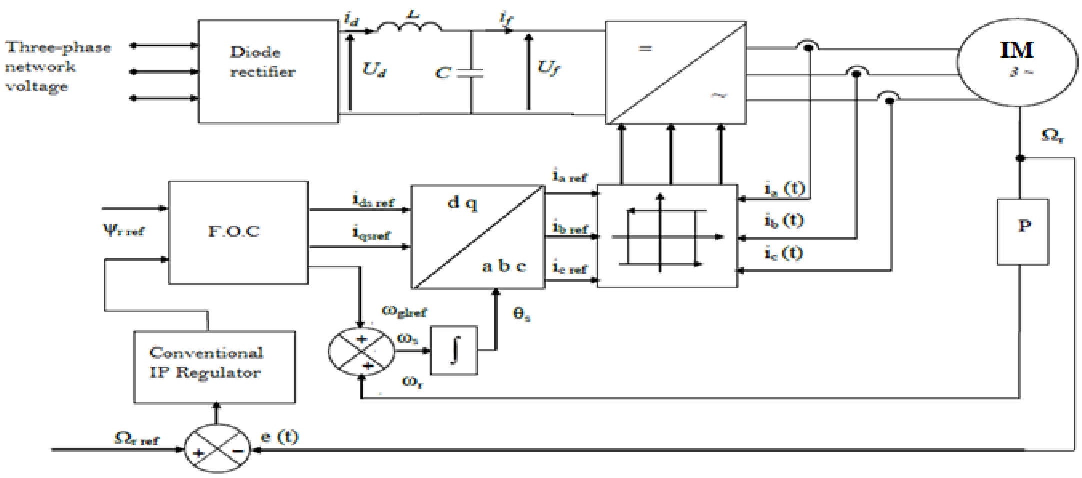

Figure 1.5: Indirect vector control of IM

1.4.6 Simulation results and discussion

To demonstrate the enhancement of the overall dynamics of the control system, various tests were conducted to evaluate the performance of the implemented control. The proportional-integral (PI) regulator was configured with the following parameters kp = 0.5 and ki=3.06 Initially, from t=0 to t=0.8 , no load was applied. Subsequently, from t=0.8 to t=1.2, a load of Cr =5N/m was introduced, resulting in a noticeable disturbance in the system The effect of Cr on the rotational speed was observed. To assess the robustness of the control system, a speed variation test was conducted from t=4 to =6 At t=8, the motor was restarted with a rotational speed of 10 tr/min.

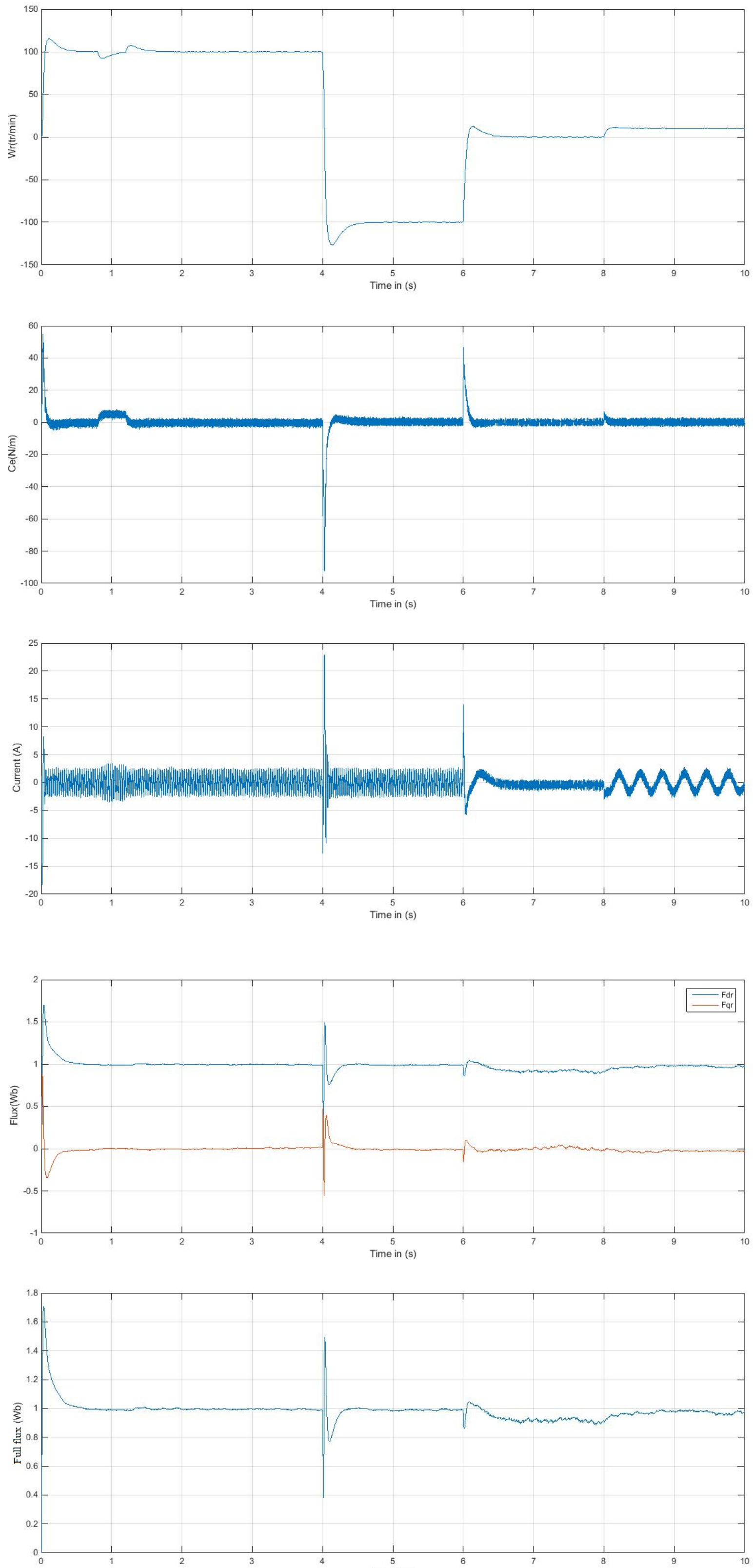

Figure 1.6: Performances IM vector control with classical PI of 1.2.

Discussion

These figures demonstrate the impact of disturbances on our system, revealing that the PI regulator's response is inadequate. Consequently, we opt to implement a fuzzy controller to assess the system's performance more effectively.

1.5 Conclusion

This chapter outlines the modeling of the induction machine (IM) and its power supply. It introduces the concept of vector control for the induction machine. Analysis of simulation results reveals that employing classical PI control for vector control of the IM yields satisfactory performance.

To bolster the robustness of IM vector control, the upcoming chapter will focus on integrating robust controllers like fuzzy logic control and synergetic control

Chapter 2

Synergetic Vector Control of Induction Motor

2.1 Introduction

Synergetic control is a method of state space formed on the basis of modern mathematics and synergetic. Russian scholar Kolesnikov puts forward it in 2000 based on the synergetic theory, used to describe and analyze the highly nonlinear and complex system of multiple subsystems To achieve this goal, one has first to choose pertinent macro-variables and then elaborate manifolds which enable the desired performance to be reached. Macro-variables can be functions of two or more state variables . First of all, it is well suited for digital control implementation, because it requires a fairly low bandwidth for the controller, a second advantage is that it operates at constant switching frequency and it does not have the chattering problems of sliding-mode control, so that it causes less power filtering problems , a third advantage is that it can help not only reduce the size of a modeled sys but also ensure the stability of the power system in general, and ease of implementation in practice highlighted this relatively new control approach..
[7]

2.2 Synergetic control

Synergetic Control Theory exploits the capability of open systems to self-organize. The theory invokes a holistic philosophy of controlled dynamic interactions between energy, matter, and information which is implemented through a combination of both positive and negative feedback. The philosophy of synergetic control is based on the principle of dynamic expansion and contraction of the state space of the controlled system. The expansion of the state space enriches the system dynamics by providing additional information which is the key to improving the performance of the closed-loop system. In contrast to the expansion, the contraction of the state space that is performed by the controller action eliminates the unwanted dynamics of the system or reduces excessive degrees of freedom. At the control design stage, these unwanted dynamics are removed by introducing dynamic constraints that are represented as invariant manifolds in the state space of the system. In order to apply the ideas of Synergetic in control theory, it is necessary to keep the conceptual correspondence to the main qualities of self organization: nonlinearity – open systems – coherence. For control tasks the most important quality is that the system must be open)[24]

2.3 The synergetic control of induction motor

Synergetic control, like Sliding Mode Control (SMC), is a technique that compels a system to follow a dynamically pre-defined trajectory as set by the designer. This method distinctively utilizes a nonlinear model to develop the control commands. The underlying principle involves meticulously shaping the system's behavior according to specific, desired dynamics, thereby ensuring robust control that is attuned to the complexities of nonlinear systems. The goal is to guide the system's evolution in a predictable and stable manner, while effectively managing the inherent nonlinearities of the system model.

$$\dot{x} = f(x, u, t) \tag{2.1}$$

where
$x = (x_1, x_2, ...x_n)$:state vector.
$u = (u_1, u_2, ...u_n)$:state vector of input control .

$f \ : \ anonlinear functionandcon - tinuousintime.$ The first step in designing a synergetic control is the formation of macro-variables defined in terms of system state variables. The macro-variable.
The command will make the system to operate on the manifold $\Psi = 0$, the dynamic evolution of the macro- variables according to the equation is defined by:

$$T\dot{\Psi} + \Psi = 0 \tag{2.2}$$

with T positive. where the function ϕ must satisfy, the following conditions to ensure the stability of this functional equation: $\Psi(0) = 0, \psi(\Psi)\Psi$ biggest then 0 for allΨ different to 0
Solution

$$\Psi(t) = \Psi_0 e^{t/T} \tag{2.3}$$

The parameter T defines the speed of convergence of macro-variables to the intersection of manifolds $\Psi = 0$.

2.3.1 Synergetic speed controller design

In this work, we propose a new robust controller design based on synergetic control [13]. The speed controller produces the reference torque Tref. The speed error is determined by

$$e(t) = \Omega_{ref} - \Omega_r = 0 \tag{2.4}$$

Consider the macro-variable given by:

$$\Psi = k_p \dot{e}(t) + k_i \tag{2.5}$$

where Kp and KI are the proportional and integral parameters of the speed macro-variable

$$\dot{\Psi} = k_p \dot{e}(t) + k_I e(t) \tag{2.6}$$

Basing on the synergetic theory, we can write:

$$T(k_p(\dot{\omega}_{ref} - \dot{\omega}_r) + k_I(\dot{\omega}_{ref} - \dot{\omega}_r)) + k_p(\omega_{ref} - \omega_r) + k_I(\omega_{ref} - \omega_r) = 0 \tag{2.7}$$

$$T^*_{em} = T_r - f_r\Omega - J(\Omega_{ref} + \frac{1}{k_p}(\dot{\frac{\Psi}{T}} + k_I(\Omega_{ref} - \Omega)) \tag{2.8}$$

The synergetic control law must ensure the stability of the closed loop speed control. One can use the following Lyapunov function:

$$V = \frac{1}{2}\Psi(e)^2 \tag{2.9}$$

after differentiation one gets

$$\dot{V} = \Psi(e)\dot{\Phi}(e) \tag{2.10}$$

2.3.2 Application of synergtic speed control for IM

To find the desired control law, the first step in the design of the synergistic control is the choice of appropriate macro-variables; in general the macro-variable can be a function of the state variables. The objective is to obtain a control law of a state function coordinate (Ω, ϕ), which provides reference values that are required for the motor speed reference Ω_{ref} and a reference flux ϕ_{ref}.

Therefore a torque control must be satisfied. The above described method to solve the problem is used, i.e. to find a control law $u(\Omega, \phi)$. The first step is the selection of macro- variables. In general the macro-variable can be any function (non-linear functions including) of state variables. We have three components ω_r, I_{ds} and I_{qs}, which allow us to impose the following invariants: technological ($\omega_r = cst$) and electromagnetic ($\phi_{dr} = cst, \Psi = 0$). [24]

2.3.3 Simulation results of the synergetic control

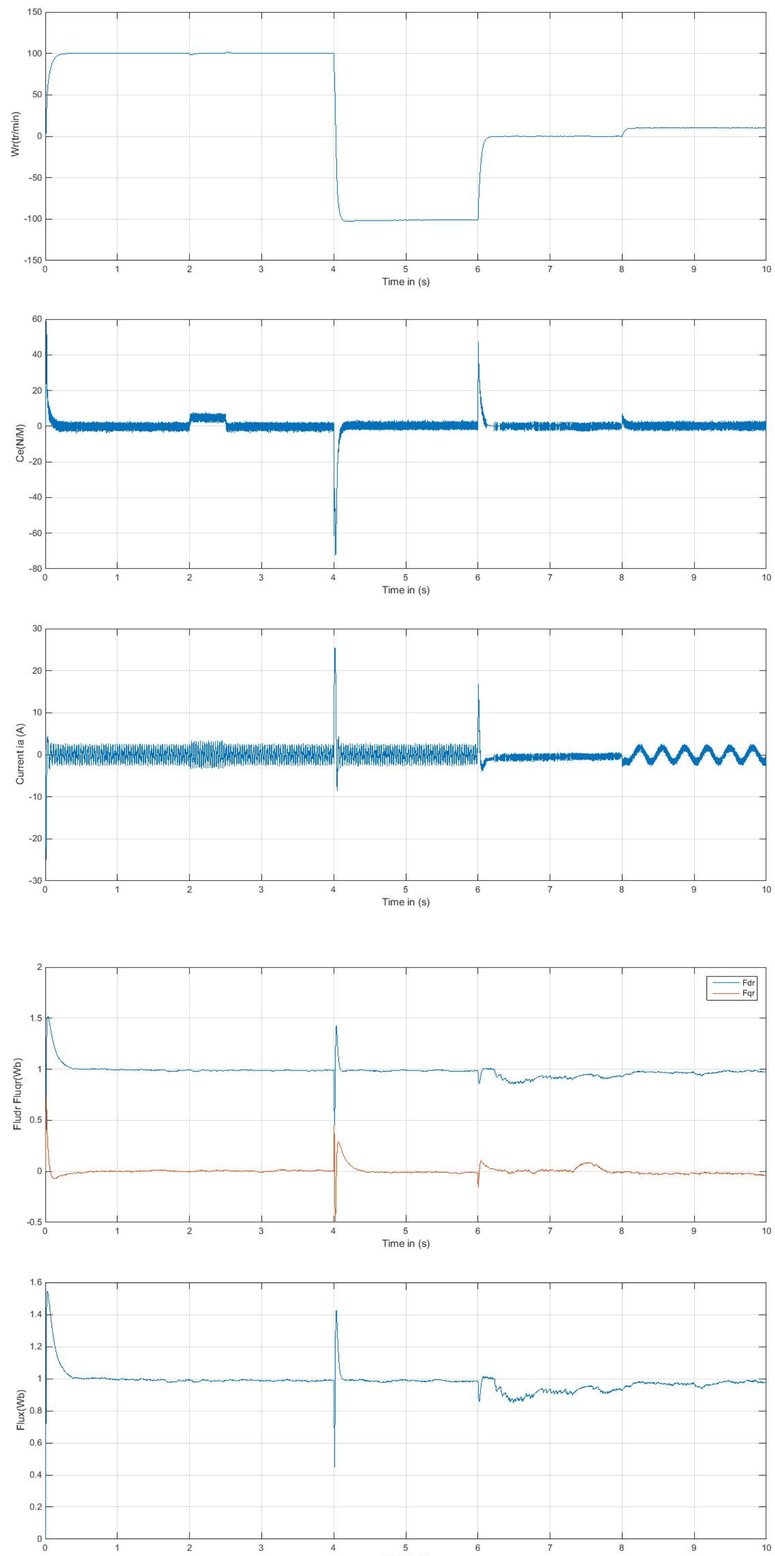

Figure 2.1: Synergetic control of induction motor

Discussion

The implementation of synergetic control in the induction motor (IM) showcases both the simplicity of its design and the enhanced performance compared to conventional and fuzzy logic regulators. Specifically, the effectiveness of the proposed synergetic control is evidenced by the nullification of the quadrature flux and performance that mirrors that of a separately excited DC machine. Moreover, synergetic control consistently delivers satisfactory outcomes, even when faced with abrupt changes in the speed reference and during the rejection of load torque disturbances.

2.3.4 Conclusion

to improve the vector control scheme of an Induction Motor (IM), a synergetic control approach was introduced. The key benefit of synergetic control lies in its ability to handle both parametric and non-parametric uncertainties, an advantage not shared by many other control strategies. Based on the results obtained, it can be stated that synergetic control enhances the robustness of the drive speed control system.

Indeed, the synergetic controller shows superior performance in terms of response time and load torque rejection. To further enhance robustness and reduce costs within the vector control scheme, the next chapter will focus on the development of a Sensorless Vector Control system for Induction Motors, employing an adaptive sliding mode observer. .

Chapter 3

Design of Improved Synergetic Sensorless Vector Control Of Induction Motor

3.1 Introduction

It is understood that high-performance commands for the induction machine can be implemented using speed/flux controllers based on field orientation concepts. Mechanical sensors such as incremental encoders and resolvers are usually employed to measure the speed of the induction machine. It is also known that the use of these sensors can lead to a reduction in the robustness and reliability of the asynchronous drive by increasing the cost and complexity of the setups. This largely explains the recent rush towards so-called sensorless controls. As stated earlier, this thesis concerns speed estimation or observation techniques for the induction machine, known as model techniques, used in a flux-oriented control, where only the stator terminals (current, voltage) are used. However, if the problem of parametric sensitivity is circumvented, these model techniques will continue to be vulnerable for low-speed state estimations.[14].

3.2 Synthesis of the Adaptive Sliding Mode Observer

sliding mode observer is illustrated in Figure. It consists of two blocks, the first concerning the machine model for state estimation (rotor flux, stator current), and the second one for the adaptation mechanism of the speed estimation [14].

3.3 Nonlinear observer

refers to a method or algorithm used in control systems to estimate the internal states of a dynamic system based on its inputs and outputs, without necessarily having direct access to these states. It utilizes mathematical models of the system dynamics and measurements of its inputs and outputs to generate estimates of the states. These observers are termed "nonlinear" when the system being observed or the observer itself exhibits nonlinear behavior. They are particularly useful in situations where direct measurement of certain states may be difficult or costly, yet accurate state information is necessary for control purposes.

The purpose of a non-linear observer is to provide accurate, real-time estimates of unmeasured or inaccessible states of a non-linear system. Non-linear observers are widely used in various fields such as control systems, robotics, aerospace engineering and many other applications where accurate estimation of system states is essential for control, effective monitoring or decision-making.

3.4 sliding mode control

The sliding mode control technique involves driving the state trajectory of a system towards a sliding surface and switching it around this surface using an appropriate switching logic until reaching the equilibrium point, hence the phenomenon of sliding. This characteristic renders the closed-loop system insensitive to parameter variations and external disturbances [Bou91]. An important property of sliding regimes is that the state trajectory in sliding mode evolves in a space of lower dimension than that of the controlled system. .

3.4.1 Theory of sliding Modes

Variable structure systems are characterized by the selection of an appropriate function and switching logic. This choice ensures the switching between these structures at any given moment. The combination of properties from each of these structures enables the imposition of the desired behavior on the overall system. [4].

3.4.2 Sliding surface

The sliding surface in sliding mode control is a mathematical representation of the desired system behavior. It is crafted to be stable and resilient to uncertainties and disturbances, directing the control input to maintain the system's state trajectories on the surface. This ensures precise and dependable control.[9].

3.5 Nonlinear observer by sliding mode

The sliding mode observer works by creating a "sliding surface" in the system state space which the error of the output estimation is equal to 0 . The main principle of the sliding mode observer is to use a discontinuous mode of operation, where the estimation of the state of the system is updated abruptly and not continuously according to the position of the sliding surface. This makes the observer robust to disturbances and model variations, as it quickly adapts to sudden changes and maintains an accurate estimate of the state of the system[5]. The observer dynamics by sliding modes refer to the state observation error

$$e = x - \hat{x} \tag{3.1}$$

Their evolution is imposed on a variety of surface, on which the error of estimation of the output

$$e = y - \hat{y} \tag{3.2}$$

Tending towards zero. Thus, the dynamics on this surface variety will be stabilized, or assigned, so as to limit or cancel the estimation error. A sliding mode observer is written in the form:

$$\dot{\hat{\epsilon}} = f(\hat{\epsilon}, u) + \Delta sign(y - \hat{y}) \tag{3.3}$$

$$\hat{y} = h(\hat{\epsilon}) \tag{3.4}$$

With

$\hat{\epsilon}$: Estimated state, size n*1.

u = Observer input or command.

y and y : $Measured and Estimated Outputs, Dimension$ p*1 $respectively.$

$where sign(y - \hat{y}) = [sign(y_1 - \hat{y}_1) \quad sign(y_2 - \hat{y}_2).....sign(y_p - \hat{y}_p)]$(3.5) V: observer gain matrix.

f(.) : Nonlinear state evolution function dimension n*1.

h(.) : Nonlinear output function dimension n*p.

The interesting properties in this type of observer are those related to the convergence in finite time towards the sliding surface or surfaces and the reduction of the total dynamics from n to n-p (n: system order, p: order of measurable outputs) conditions on the sliding surface.

The robustness vis-à-vis internal (parametric) and external disturbances (load, noise, etc.) will be conferred to the optimal settings of the sign function gains where a chattering–performance compromise (chattering) should be observed.

3.6 Adaptive sliding mode observer

The sliding mode observer is illustrated in Figure. It consists of two blocks, the first concerning the machine model for state estimation (rotor flux, stator current), and the second one for the adaptation mechanism of the speed estimation [6].

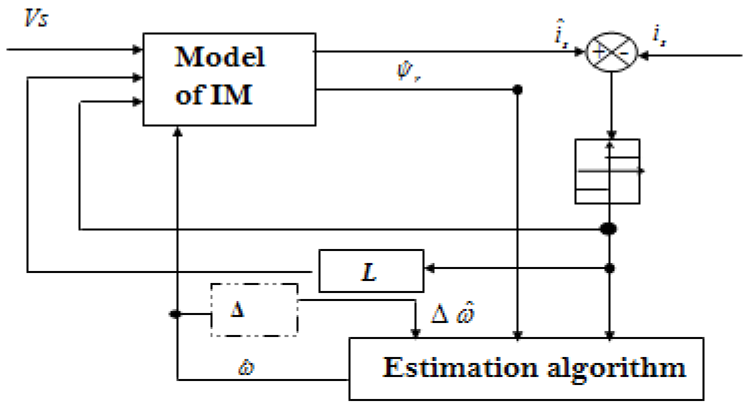

Figure 3.1: Structure of an observer by adaptive sliding modes.

3.6.1 Conception of sliding mode observer

The sliding-mode observer consists of stabilizing the error dynamics of the states to estimate which amounts to :

- Determine a sliding surface on which the error of the output estimate is zero.
- Establish the sliding conditions (calculation of the observer gains for which all system trajectories move towards and remain on the sliding surface (attractiveness) (invariance).

The observer is designed from the model of the stator-bound induction motor so the sliding surfaces are defined by:

$$[s] = \begin{bmatrix} s_1 \\ s_2 \end{bmatrix} = \begin{bmatrix} \hat{i}_{s\alpha} - i_{s\alpha=} \\ \hat{i}_{s\beta} - i_{s\beta} \end{bmatrix}$$

The formulation of the motor condition model given by:

$$\frac{dx}{dt} = Ax + Bv_s \tag{3.6}$$

$$\frac{d\hat{x}}{dt} = \hat{A}\hat{x} + Bv_s + ksign(\hat{i_s} - i_s) \tag{3.7}$$

with $\hat{x}$:is the estimated state of the x state (assumed true). $\hat{x} = [\hat{i_s}\hat{\psi_r}]^T$; $\hat{i_s} = [\hat{i_{s\alpha}i_{s\beta}}]^T$; $\hat{\psi_r} = [\hat{\psi_{r\alpha}\psi_{r\beta}}]^T$; $v_s = [v_{s\alpha}v_{s\beta}]^T$

$$[K] = \begin{bmatrix} k_1 \\ -Lk_1 \end{bmatrix} : Gain \quad matrix$$

where

$$[K] = \begin{bmatrix} -k_1 & 0 \\ 0 & -k_2 \end{bmatrix}$$

$$[L] = \begin{bmatrix} l_{11} & l_{12} \\ l_{21} & l_{22} \end{bmatrix}$$

then the error status model is given as follows:

$$\frac{de}{dt} = A_e + \Delta A\hat{X} + Ksign(\hat{i_s} - i_s) \tag{3.8}$$

with

$e = \hat{x} - x = [e_i e_\phi]^T$: stat error
$\Delta A = \hat{(}A) - A$:modelling error
$e_i = \hat{i_s} - i_s$: current error
$e\psi = \hat{\psi} - \psi_r$: flux error
Δ A $= \begin{bmatrix} \Delta A_{11} & \Delta A_{12} \\ \Delta A_{21} & \Delta A_{22} \end{bmatrix}$: matrix block.

The conditions of the slide mode, in terms of convergence to the surface and invariance on the same surface, allow to write:

$e_i = 0, \frac{de_i}{dt} = 0$

And so the state equation (2.7) becomes:

$$0 = A_{12}e_\psi + \Delta A_{11}\hat{i}_s + \Delta A_{12}\hat{\psi}_r - z \tag{3.9}$$

$$\frac{d}{dt}e_\psi = A_{22}e_\psi + \Delta A_{21}\hat{i}_s + \Delta A_{22}\hat{\psi}_r + Lz \tag{3.10}$$

with
$z = -k_1 sign(\hat{i_s} - i_s)$:switching function.

The modeling error, or A variation, is considered to be due to the variation of the parameter alone ω, hence the recovery of the same formulations:

$\Delta A = \begin{bmatrix} o & \frac{\Delta\omega}{\epsilon}J \\ 0 & \Delta\omega J \end{bmatrix}$:$\Delta\omega = \hat{\omega} - \omega$; J= $\begin{bmatrix} 0 & -1 \\ 1 & 0 \end{bmatrix}$ then

$$0 = A_{12}e_\psi - \frac{\Delta\omega}{\epsilon}J\hat{\Psi}_r - z \tag{3.11}$$

$$\frac{d}{dt}e_\psi = A_{22}e_\psi - \Delta\omega J\hat{\psi}_r + Lz \tag{3.12}$$

$$e_\Psi = \frac{\Delta\omega}{\epsilon} {A_{12}}^{-1} J\hat{\psi}_r + {A_{12}}^{-1} z \tag{3.13}$$

$$\frac{d}{dt} e_\psi = A_{22}(\frac{\Delta\omega}{\epsilon} J\hat{\psi}_r {A_{12}}^{-1} + {A_{12}}^{-1} z) + \Delta\omega_r J\hat{\psi}_r + Lz \tag{3.14}$$

we have

$A_{22} = -\epsilon A_1 2$

$$\frac{e\psi}{dt} = V k_1 sign(e_i) \tag{3.15}$$

with $V = (L - \epsilon I)$ and $\epsilon = \frac{\sigma L_s L_r}{M}$ For the determination of k_1 and k_2 the Popov condition $S * \dot{S}$ must be checked to ensure the stability of the flow observer. Therefore it is necessary to explain first of all the equation of the current error in the following form[4][18]:

$$\frac{d}{dt}\begin{bmatrix} e_1 \\ e_2 \end{bmatrix} = \begin{bmatrix} -\gamma_1 & 0 \\ 0 & -\gamma_1 \end{bmatrix}\begin{bmatrix} e_1 \\ e_2 \end{bmatrix} + \begin{bmatrix} \gamma_2 & \gamma_3 \\ -\gamma_3 & \gamma_2 \end{bmatrix}\begin{bmatrix} e_3 \\ e_4 \end{bmatrix} + \begin{bmatrix} -k_1 sign(e_1) \\ -k_2 sign(e_2) \end{bmatrix}$$

with

$\gamma_1 = \frac{R_s}{\sigma L_s} + \frac{M^2}{\sigma L_s L_r}\sigma_r$ $\gamma_2 = \frac{M}{\sigma L_s L_r}\sigma_r$ $\gamma_3 = \frac{pM}{\sigma L_s L_r}\Omega$

3.6.2 Determining the gains matrix L

$$|\psi_{r\alpha}| < \eta_1 \quad and \quad |\psi_{r\beta}| < \eta_2 \tag{3.16}$$

$$\rho_1 > (\frac{R_s}{\sigma L_s} + \frac{M^2\sigma_r}{\sigma L_s L_r})|e_1| + \frac{M\sigma_r}{\sigma L_s L_r}(\eta_1 + |\hat{\psi}_{r\alpha}|) + \frac{PM}{\sigma L_s L_r}|\Omega_r|(\eta_2 + |\hat{\psi}_{r\beta}|) \tag{3.17}$$

$$\rho_2 > (\frac{R_s}{\sigma L_s} + \frac{M^2\sigma_r}{\sigma L_s L_r})|e_2| + \frac{M\sigma_r}{\sigma L_s L_r}|\Omega_r|(\eta_2 + |\hat{\psi}_{r\beta}|) + \frac{PM}{\sigma L_s L_r}|\Omega_r|(\eta_1 + |\hat{\psi}_{r\alpha}|) \tag{3.18}$$

$$L = -\gamma A_{12}^T + \epsilon I \tag{3.19}$$

The development of this relationship leads to:

$$L = \begin{bmatrix} -\epsilon - \frac{\gamma\sigma_r}{\epsilon} & \frac{\gamma\omega_r}{\epsilon} \\ -\frac{\gamma\omega_r}{\epsilon} & -\epsilon - \frac{\gamma\sigma_r}{\epsilon} \end{bmatrix}$$

To achieve the targeted dynamic performance of rotor flux estimation, the matrix L could be transcribed as followss:

$$L = \begin{bmatrix} -(q-1)\epsilon - \frac{\gamma\sigma_r}{\epsilon} & \frac{\gamma\omega_r}{\epsilon} \\ -\frac{\gamma\omega_r}{\epsilon} & -(q-1)\epsilon - \frac{\gamma\sigma_r}{\epsilon} \end{bmatrix}$$

q: is a positive constant chosen to ensure convergence and achieve the desired performance (dynamic and static) for the estimated rotoric flux[1][22][15].

3.7 concepion of proposed adaptative sliding mode

The speed estimation based on nonlinear observer like sliding mode observer seems an interesting choice, in sense of robustness against parameter deviation, and rapid convergence [2][11]

However, the classical SMO has main drawback such that the observed quantities include high frequency. This latter is provide by discontinuous condition input results in electromagnetic torque high fluctuations which excites the high unmodeled dynamics or mechanical resonances[11] .

To overcome this problem, various solutions have been proposed in order to make a compromise between the chattering phenomenon minimization and observer robustness. In reference [23] a first order and second order SMO are presented, the chattering phenomenon was reduced however low pass filter causes unpredictable time delays in the estimated values which need a compensation technique.

In this study, we propose a simple but powerful improved sliding observer (ISMO) witch able to reduce the chattering phenomena, and keep the advantages obtained in the classical SMO. The suggested observer utilizes single input which is the stator current error.The proposed ISMO not only improves the accuracy tracking performance with chattering free and robustness against parameter variations, but also assure good speed estimation at very low speed.

3.7.1 Design of suggested improved adaptive sliding-mode observer

Theimproved adaptive sliding-mode observer explained here is a modification of the sliding-mode observer (eqn.1), where the switching observer term $sign(\hat{i}_s - i_s)$,

has been replaced by smooth function. The error between estimated stator current and measured current i.e sliding surface $e_1 = \hat{i}_{s\alpha} - i_{s\alpha}$, $e_2 = \hat{i}_{s\beta} - i_{s\beta}$

are considered as variables of smooth function, this later is introduced in SMO replacing

the discontinuity observer term. The discontinuity term was replaced by sigmoid and smooth function in reference given by:

$$U_i = \frac{K_\omega}{\lambda} S(\omega) \qquad \text{if} \qquad |S(\omega)| < \lambda \tag{3.20}$$

Hence the equation (III.) can be expressed by:

$$\frac{d\hat{x}}{dt} = \hat{A}\hat{X} + BV_s + U_i \tag{3.21}$$

where ui(i=1,2) is FI output. In this case, the estimated speed is given by:

$$\hat{\omega} = \int_0^t \gamma\, \mu\, (U_1 \hat{\psi}_{r\beta} - U_2 \hat{\psi}_{r\alpha}) dt \tag{3.22}$$

3.7.2 Simulation results and discussion

To investigate the effectiveness of the proposed system, and to check the closed-loop stability of the complete system, several tests were performed at different dynamic operating conditions such as sudden change in command speed, and step change in load

In order to demonstrate the viability of the suggested ISMO, several simulation tests of the diagram bloc shown in Fig. 3 were performed for a variety of operating conditions. The data parameters of the test motor are reported in Table I. The simulation responses of drive system with ISMO are shown in Fig.3 (a), and those with conventional SMO in Fig.3(b).

In first stage, to assess the performance and the robustness of ISMO, we start with comparison between proposed ISMO and classical SMO

It's remarked the rapid response of the estimated speed in transients. Also, the estimated speed has much less chattering. The simulation tests at low speed have been also investigated by speed reverses at rated load, respectively, at (Fig.) $\omega_r^* = \pm 100$ (rad/s) , and ω_r^* ± 50 (rad/s) and $\omega_r^* = \pm 25$(rad/s) .The proposed observer is still able to maintain estimates in those operating conditions and the dynamic behaviour is acceptable.

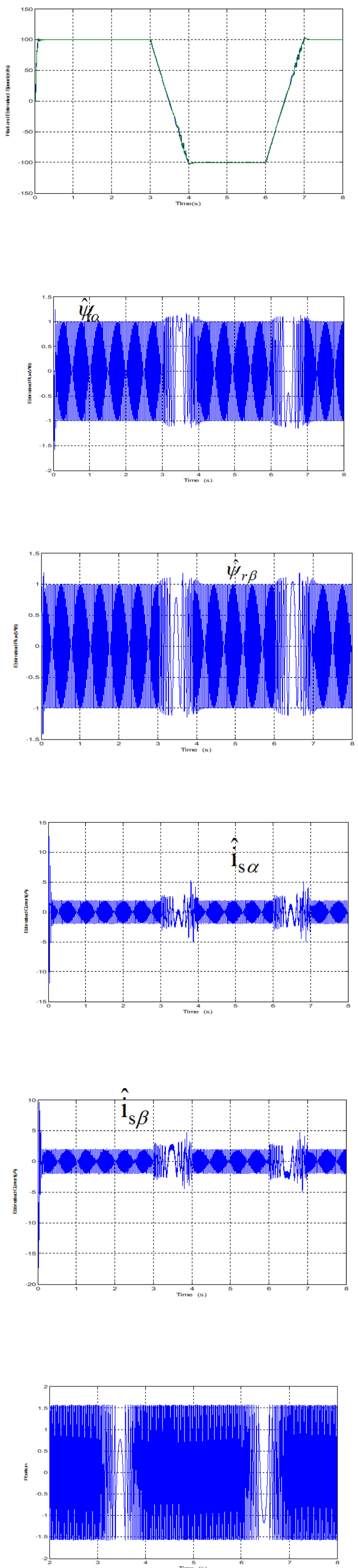

(a) Simulation results of ISMO.

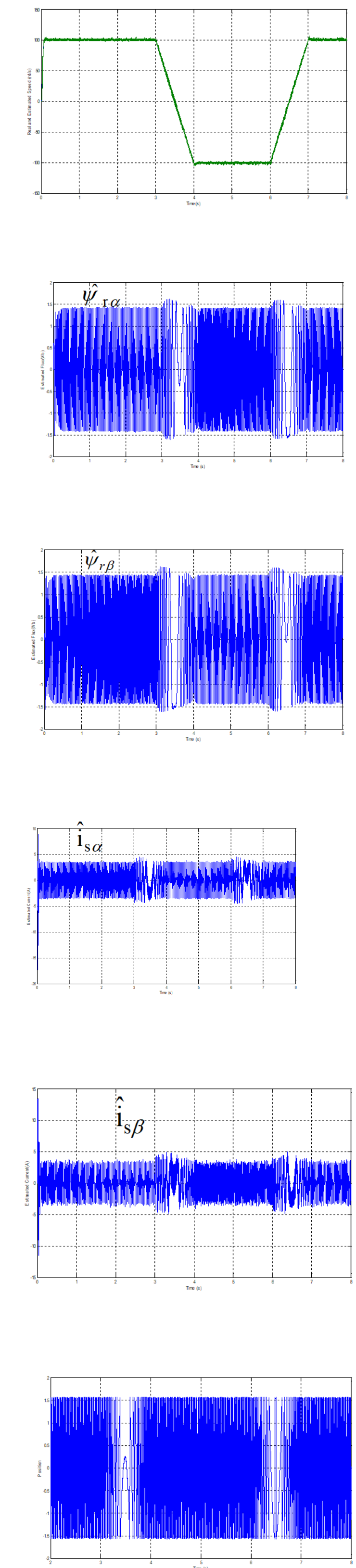

(b) Simulation results of SMO.

Figure 3.2: Transient response due to trapezoidal speed command ±100 (rad/s).

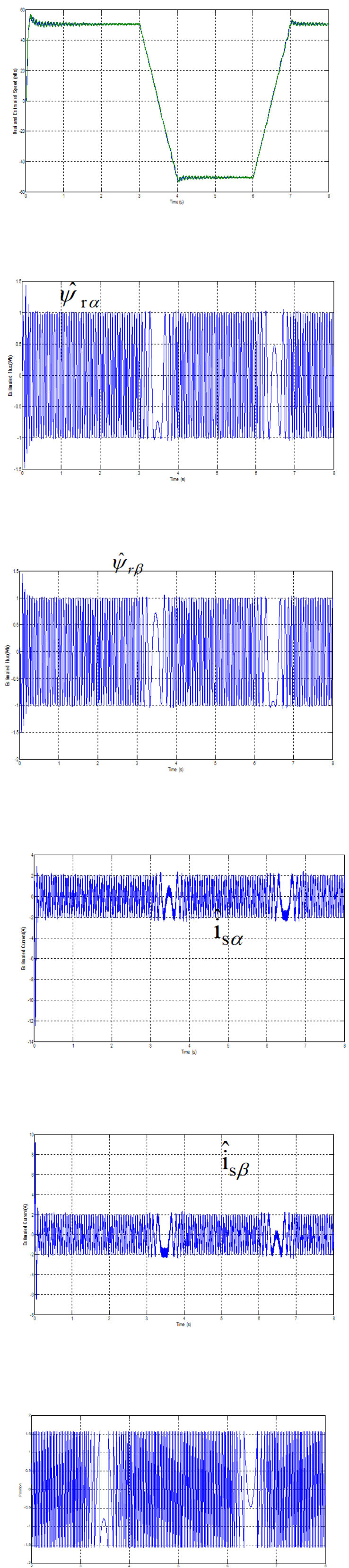

(a) Simulation results of ISMO.

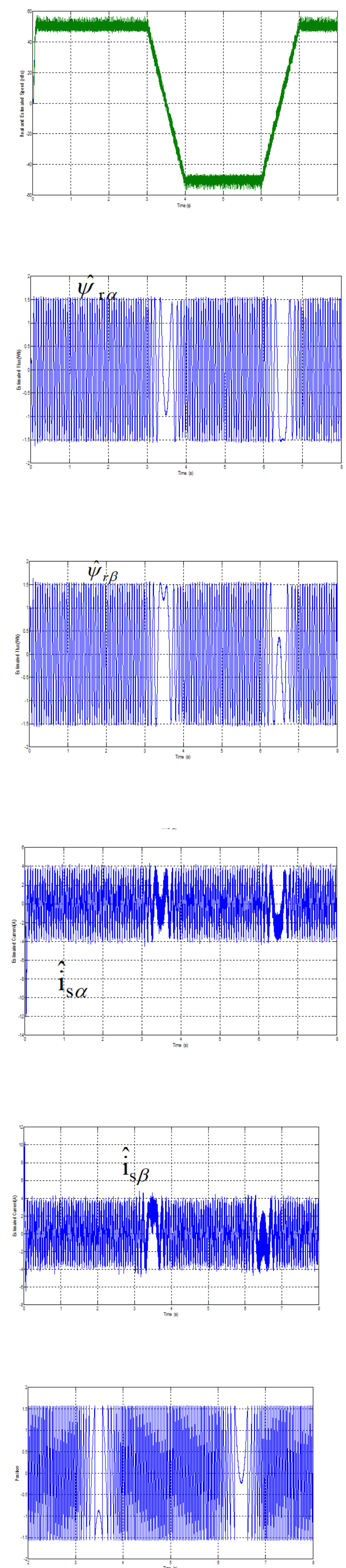

(b) Simulation results of SMO.

Figure 3.3: Transient response due to trapezoidal speed command ±50 (rd/s).

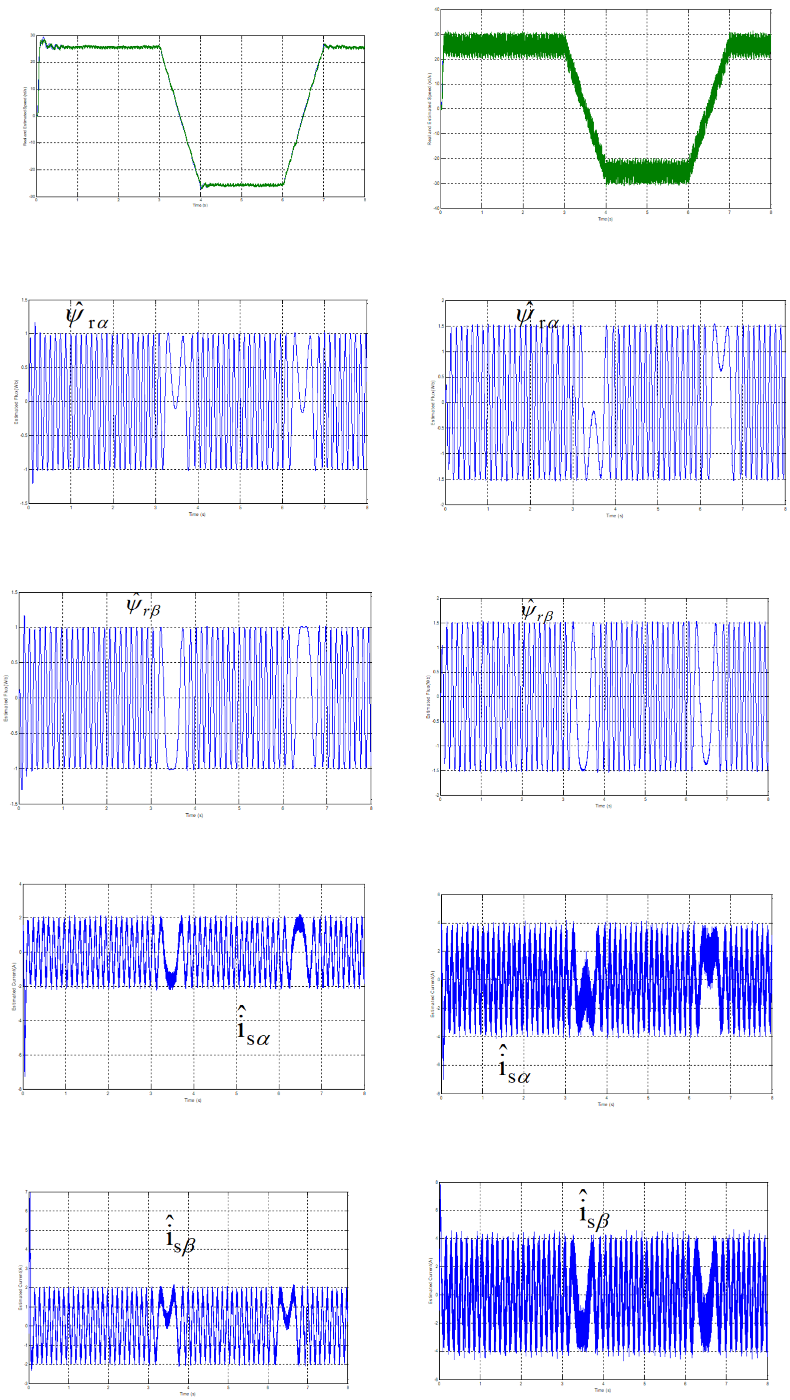

(a) Simulation results of ISMO. (b) Simulation results of SMO.

Figure 3.4: Transient response due to trapezoidal speed command ±25 (rd/s).

3.7.3 Speed Maximum Dynamic Error

The effectiveness of the sensorless scheme in terms of the speed estimation accuracy are also tested and compared to those of the algorithm proposed . Figures (3) show the maximum of the speed dynamic error versus the speed reference, it can be noted that the accuracy of the speed estimation is considerably improved. In fact in the case of the proposed algorithm the dynamic error is 0.35% at a very low speed of (5 rad/s)no load and doesn't exceed 0.21% at the rated speed (100 rad/s) see figure(3.5), against a dynamic error of 0.55 percent at (5rad/s), and 0.22 percent speeds of the algorithm From the obtained results, it can be concluded that a simple modification of the speed estimation algorithm , can improve greatly the speed estimation accuracy particularly at very low speeds. is 1.21% at a very low speed of (5 rad/s) with load and doesn't exceed 0.3% at the rated speed (100 rad/s) see figure (3.6).

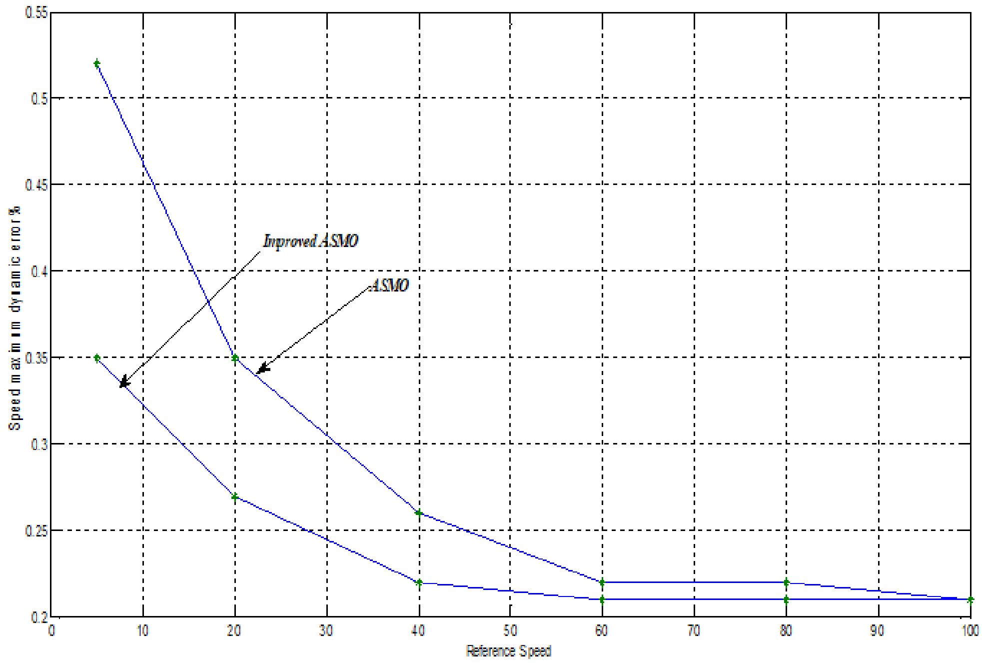

Figure 3.5: Speed maximumdynamic error at no load operation Versus reference speed.

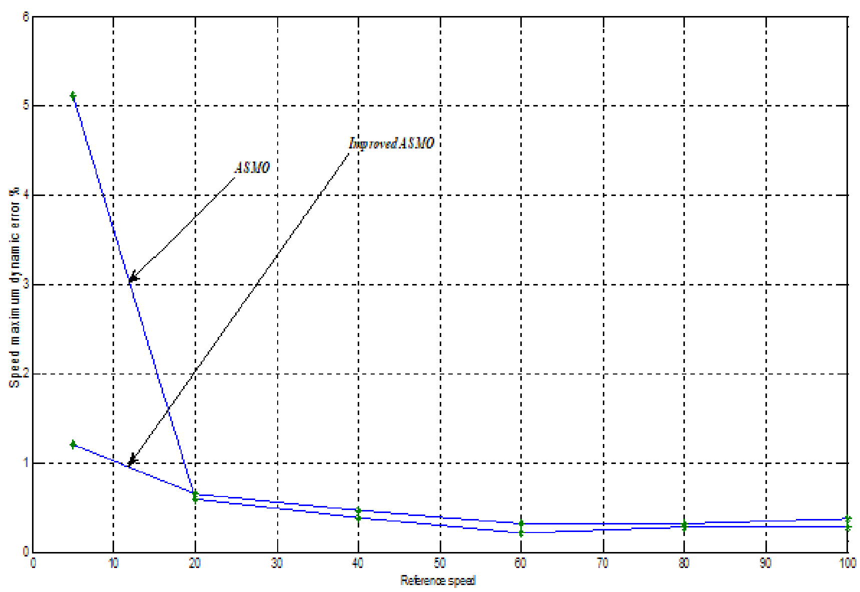

Figure 3.6: Speed maximum dynamic error at load operation Versus reference speed.

3.7.4 Conclusion

In order to reduce the chattering phenomena of conventional adaptive sliding-mode observer, it was proposed in this chapter a simple but powerful improved sliding observer (ISMO) witch able to reduce the chattering phenomena, and keep the advantages obtained in the classical SMO. The suggested observer utilizes the stator current error and smooth. function to replace the switching term . From obtained simulation results, one can seen that The proposed ISMO has given good estimation accuracy with free chattering even at very low speed.

GENERAL CONCLUSION

The study carried out during this memory work focused on implementation of an improved synergetic sensorless decoupled control of induction motor based on an adaptive sliding mode observer.

The features of presented sensorless scheme in terms of the speed estimation accuracy has been examined even at low speed operations, and for reference speed variation. In high performance applications, the induction motor is controlled via vector control technique. The basic idea of this technique is to decompose the stator current vector into two components: one used to control the machine flux and the other to adjust torque, hence the control of torque and the flux is independently.

However, vector control needs accurate speed and flux measurement or estimation for the high performance of IM drives. The measurement process is fraught with difficulties, particularly the high cost and fragility of the sensors. Furthermore, the physical environment does not always permit the use of sensors. So the sensorless control seems good solution for costs reduction, and solving several of the implementation problems encountered: lack of space, severe environment.

To do this, the first chapter of this work was devoted to modelling of IM using Park model, and application of decoupled control strategy to IM. At the end of chapter the main performance of vector control were illustrated by the simulation results.

The use of vector controlled IM drives yields various advantages over DC motors in terms of low cost, size, robustness, no maintenance. However, the vector control of IM needs the employ of an accurate shaft encoder for good operating. Hence the sensorless control seems good solution for costs reduction, and solving several of the implementation problems encountered: lack of space, severe environment.

We have dedicated the second chapter, to present the theory of fuzzy logic, and synergetic control applied to IM. These two controls provide high performances in terms of tracking and robustness. The presented control approaches were justified by the numeral results.

In order to reduce the cost of the control by eliminating the speed sensor, and enhanced the accuracy estimation spatially at low speed, an improved adaptive sliding-mode observer for speed-sensorless control of IM was developed. The presented observer estimate the rotor flux components in the stationary reference frame from IM. The speed is detected by adding a Lyapunov function. The performance of suggested observer was illustrated by simulation results.

Regarding the continuation of this work, different perspectives open up:

-Development of integral fractional observer for of IM
- Design of sensorless fault tolerant control of IM
- Conception intelligent decoupled control of IM using internet of things
- Practical realization of the proposed control strategy.

Bibliography

[1] I. Al-Rouh. *Contribution à la Commande sans Capteur de la Machine Asynchrone*. PhD thesis, Henri Poincaré University, Nancy-I, France, 2004.

[2] H. Allamehzadeh and J.-Y. Cheung. Robust fuzzy control with sliding mode property and inherent boundary layer. In *Proceedings of the International Conference on American Control*, pages 4231–4236, 2003.

[3] H. Amimeur. *Contribution au contrôle de la machine asynchrone double étoile*. PhD thesis, University of Batna, Batna, Algeria, 2012.

[4] A. Aoufi. Utilisation d'observateurs à modes glissants pour le contrôle direct de couple et le contrôle vectoriel d'une machine asynchrone à cage. Master's thesis, Institution where the thesis was conducted.

[5] H. Bouchareb. Observateur non linéaire mode glissant. Magister thesis, 2021.

[6] T. Boukhobza. *Contribution aux Formes d'Observabilité pour les Observateurs à Modes Glissants et Étude des Commandes par Ordres Supérieurs*. PhD thesis, University of South Paris, Orsay, 1997.

[7] M. Boumegouas and K. Kouzi. A new synergetic scheme control of electric vehicle propelled by six-phase permanent magnet synchronous motor. *Journal Name*, Volume Number(Issue Number):Page Numbers, 2020.

[8] M. K. B. Boumegouas, K. Kouzi, and M. Birame. Robust synergetic control of electric vehicle equipped with an improved load torque observer. *International Journal of Emerging Electric Power Systems*, 2023.

[9] Faucher. *Les Plans d'Expériences pour Le Réglage de Commandes à Base de Logique Floue*. PhD thesis, Institut National Polytechnique de Toulouse : Electrical Engineering and Automation, Septembre 2006.

[10] H. Guermit, K. Kouzi, and S. A. Bessedik. Novel design of an optimized synergetic control for dual stator induction motor. *COMPEL - Int. J. Comput. Math. Electr. Electron. Eng.*, 38(6):1828–1845, Oct. 2019.

[11] K. Hongryel, S. Jubum, and L. Jangmyung. High speed sliding mode observer for the sensorless speed control of a pmsm. *IEEE Transactions on Industrial Electronics*, 58(9):4096–4107, 2011.

[12] N. Khalil. *Contribution à la Commande de la Machine Asynchrone par DTC et Logique Floue*. PhD thesis, Université de Constantine, Constantine, Algeria, 2006.

[13] I. Kondratiev and R. Dougal. General synergetic control strategies for arbitrary number of paralleled buck converters feeding constant power load: Implementation of dynamic current sharing. *Journal Name*, Volume Number(Issue Number):Page Numbers, 2006.

[14] K. Kouzi. Contribution des techniques de la logique floue pour la commande d'une machine à induction sans transducteur rotatif. Master's thesis, University of Elhadj Lakhdar, Batna, Algeria.

[15] K. Kouzi, L. Mokrani, and M.-S. Naït-Saïd. Adaptive sliding-mode observer for speed-sensorless control of induction motors. *IEEE Transactions on Industry Applications*, 36(5):1380–1387, 2000.

[16] K. Kouzi, L. Mokrani, and M.-S. Naït-Saïd. A new design of fuzzy logic controller with fuzzy adapted gains based on indirect vector control for induction motor drive. In *IEEE-SSST Annual Meeting*, West Virginia, USA, March 2003.

[17] K. Kouzi, L. Mokrani, and M.-S. Naït-Saïd. High performances of fuzzy self-tuning scaling factor of pi fuzzy logic controller based on direct vector control for induction motor drive without flux measurements. In *Proceedings of the IEEE International Conference on Industrial Technology (ICIT)*, December 2004.

[18] K. Kouzi, L. Mokrani, and M.-S. Naït-Saïd. A rotor flux sliding-mode observer for a fuzzy logic control of direct field oriented induction motor. In *International Conference on Electrical and Electronics Engineering*, Sétif, October 2004.

[19] K. Kouzi and M.-S. Naït-Saïd. Adaptive fuzzy logic speed-sensorless control improvement of induction motor drives for standstill and low speed operations. *International Journal COMPEL*, 26(1):22–33, Jan 2007.

[20] H. Tajima, G. Guidi, and H. Umida. Consideration about problems and solutions of speed estimation method and parameter tuning for speed-sensorless vector control of induction motor drives. *IEEE Transactions on Industry Applications*, 38(5):1282–1289, Sept./Oct. 2002.

[21] M. Tursini, R. Petrella, and F. Parasiliti. Adaptive sliding-mode observer for speed-sensorless control of induction motors. In *IEEE International Conference on Systems, Signals and Devices*, 2000.

[22] M. Tursini, R. Petrella, and F. Parasiliti. Adaptive sliding-mode observer for speed-sensorless control of induction motors. *IEEE Transactions on Industry Applications*, 36(5):1380–1387, Sep./Oct. 2000.

[23] C. Vasilios. Pmsm sensorless control on sliding mode observers methodology for nonlinear system with model imprecision. In *International Workshop on Recent Advances in Sliding Modes (RASM)*, 2015.

[24] A. Yahi and L. Barazane. Improving speed performances of induction motor by using synergetic control theory. *Journal Name*, Volume Number(Issue Number):Page Numbers, 2020.

[25] A. Zorig, A. Belkheiri, M. Belkheiri, and K. Kouzi. Adrc control of an induction motor with varying parameters. In *19th International Multi-Conference on Systems, Signals & Devices (SSD)*, 2022.

Appendix A

Appendix A

Table A.1: Motor Specifications

Parameter	**Value**
Number of pole pairs	2
Rated power (kW for 50 Hz)	0.75
Nominal speed (tr/min)	1400
Nominal voltage (V)	220/380
Nominal current (A)	3.6/2.1
Nominal torque (Nm)	5
Rs; Rr (Ω)	10; 6.3
Ls; Lr (H)	0.656; 0.653
M (H)	0.612
J (kg.m^2)	0.02
fs (N m.s)	0

- Three phase Network parameter: 220/380 V ; 50Hz.
- Inverter parameter:$\Delta_i = 0.1A$ Hysteresis strip.
- Filter parameter : Capacity C=6.10$^{-3}F, Inductance L = 1.2.10^{-3}H$.